

Gauge Block Calibration by Optical Interferometry at the National Research Council of Canada*

J. E. Decker and J. R. Pekelsky
Dimensional Metrology Program
Institute for National Measurement Standards (INMS)
National Research Council Canada (NRC)
Ottawa, CANADA K1A 0R6

Abstract

The definition of the SI unit for length, the metre, is the length of the path travelled by light in vacuum during a time interval of $1/299\,792\,458$ of a second. Optical interferometry offers a measuring method to determine the number of wavelengths of light that span the length of the gauge block. The instrumentation and methods developed at the National Research Council of Canada (NRC) for this specialized interferometric technique are described. Also discussed are the details of the measurement procedure. An outline of the uncertainty attributed to this system is evaluated in accordance with the ISO *Guide to the Uncertainty in Measurement*. Finally, planned improvements to the NRC system are briefly described.

1 Introduction

The Institute for National Measurement Standards (INMS) at the National Research Council Canada (NRC) maintains primary standards in most of the measurement domains of the International System of Units (SI). In the area of length metrology, the SI metre is defined as the length of the path travelled by light in vacuum during a time interval of $1/299\,792\,458$ of a second. NRC realizes the definition of the metre by performing dimensional measurements using the technique of optical interferometry with wavelengths of radiations recommended in the CIPM *Mise en Pratique for the Definition of the Metre* [1]. The primary standard for length at NRC is the radiation emitted by an iodine-stabilized 633 nm He-Ne laser, operated in accordance with the *Mise* guidelines. Gauge blocks are the material artifacts that provide traceability to the definition of the metre — the first link in the chain of transfer standards for industry.

Quality manufacturing is continually challenging high-accuracy gauge block measurement as dimensional tolerances on parts continually become tighter. Highest grade gauge blocks require best up-to-date measurements to keep up with the demands of industry. Tolerances are now measured in 10's of nanometres

*presented at the **Measurement Science Conference** Pasadena, California, 23–24 January 1997; NRC Internal Report No. 40002

and there is pressure on measurement capabilities to provide this level of uncertainty. This push for lower uncertainties has driven the modernization of the gauge block calibration facilities at NRC.

Investigations into interferometric gauge block measurement at NRC began in 1936 in the length standards group. Several interferometric instruments were developed in the following years in support of the gauge measurement facility, spurred on by the second world war [2]. One such instrument, a Fizeau interferometer, illuminated with isotope lamps built in-house [3], was very successful, and is still used today for quick gauge inspection. In 1955, a research-grade instrument was constructed to improve short gauge block throughput and facilitate the calibration of long bars. This instrument was completely redesigned in the late 1970s to accommodate improvements in the measurement process as a result of the many years of experience and evolving technology. This round of modifications was completed in the early 1980s, in which interference fringe measurement became enhanced with computer and video additions and remote operation of components.

Research into optical radiation sources for length measurement was done in parallel with the development of gauge block interferometry at NRC [4]. Earlier research concentrated on the fabrication and characterisation of cadmium-114, mercury-198 and krypton-86 lamps [5]. The iodine-stabilised He-Ne laser was invented at the NRC in 1969 by Hanes [6, 7], who was the first to observe the iodine hyperfine structure in saturated absorption at 633 nm, measure the component wavelengths, and suggest that a laser stabilised on an iodine resonance might be suitable as a new primary standard of length. Corroboration by researchers at other labs led to its ultimate adoption as a recommended radiation by the CIPM.

In this paper, the instrumentation and method of absolute gauge block measurement by optical interferometry currently in use at NRC is described. The measurement uncertainties associated with the interferometric gauge block calibration and planned improvements at NRC are briefly discussed.

2 Gauge Block Measurement Process

The following is a general model of the gauge block measurement process, which influences the design parameters of the apparatus and methodology.

2.1 Definition of Gauge Length

The exact definition of the length of a gauge block is “the distance from the centre of the first face of the block to the plane of the reference flat to which the opposite face of the block is wrung, so as to include the wringing film” [8], as shown in Figure 1. Wringing is discussed below in §4.1.

Gauge blocks are made within a few micrometres or less of their nominal length L (the value marked on the side of the block), so it is convenient to express gauge block length ℓ , as a deviation d , where

$$\ell = L + d. \tag{1}$$

Positive d indicates that the length of the gauge is longer than the nominal length and negative d indicates that it is shorter. The grade of gauge blocks made for interferometric measurement are high quality, which means that the deviation from nominal length is very small (< 100 nm) and the gauges also have excellent flatness, parallelism, and surface finish qualities. The interferometric technique demands that only new-condition gauge blocks be used.

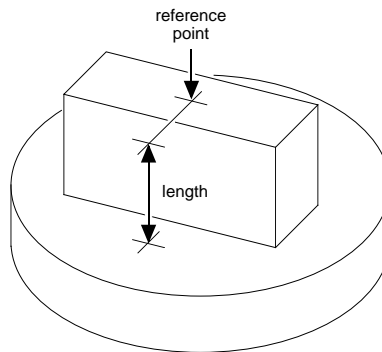


Figure 1: Definition of the length of a gauge block.

2.2 The Method of Excess Fractions

The *Mise in Pratique* lists radiations that can be used to define the metre, and assigns a value to each of the radiations, wavelength λ , and its corresponding uncertainty $u(\lambda)$. These light waves can be used to measure the length of a gauge block by counting how many waves m it takes to span the length of the gauge (see Figure 2),

$$m\lambda = 2\ell. \quad (2)$$

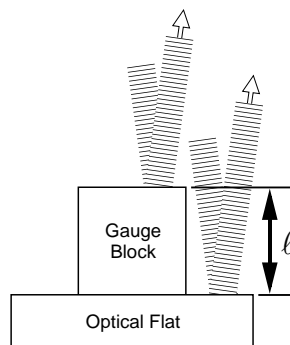


Figure 2: Portrayal of light reflecting from the top of the gauge block, and the top surface of the optical flat. The optical path difference is twice the height of the block, or 2ℓ .

If ℓ is an exact multiple of λ , then m is an integer. In general, however, λ is not an aliquot of ℓ , and so m is a mixed fraction. For example,

$$\begin{aligned} \ell = 100 \text{ mm}, \lambda_1 = 633 \text{ nm} &\rightarrow m_1 \approx 315\,955.766 \\ \lambda_2 = 612 \text{ nm} &\rightarrow m_2 \approx 326\,797.386 \\ \lambda_3 = 543 \text{ nm} &\rightarrow m_3 \approx 368\,324.125. \end{aligned}$$

Some scanning instruments can move a sensor from one end to the other, and literally count the waves

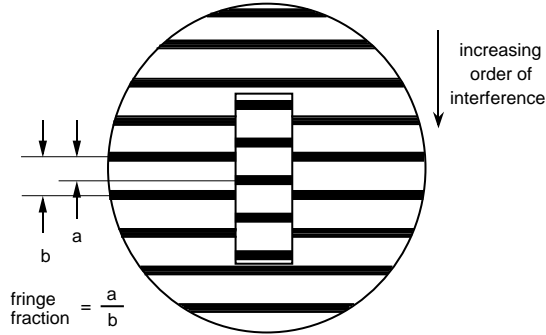


Figure 3: Schematic diagram of fringe fraction measurement. The figure depicts an interference pattern arising from a gauge block wrung to an optical flat, as viewed from above in the gauge block interferometer.

spanning ℓ , *i.e.*, count m . Another approach (the basis of the NRC instrument) arranges to form a static interference pattern so that the difference between reflection from the near and far surfaces can be viewed as a relative shift in the fringes (see Figure 3). If m is an integer, then there is no pattern shift, but if m has a fractional component, there is a corresponding shift in the fringe pattern. This shift is called the “fringe fraction.” Note that the fringe pattern tells us nothing about the number of integral waves spanning ℓ , only the fractional part. Nonetheless, the fraction is a characteristic of ℓ and λ .

If we perfectly measure, one at a time, the characteristic fraction $F_1, F_2, F_3, \dots, F_n$ for each of several wavelengths $\lambda_1, \lambda_2, \lambda_3, \dots, \lambda_n$ as in the previous example,

$$\begin{aligned} \ell = 100 \text{ mm}, \lambda_1 = 633 \text{ nm} &\rightarrow F_1 \approx 0.766 \\ \lambda_2 = 612 \text{ nm} &\rightarrow F_2 \approx 0.386 \\ \lambda_3 = 543 \text{ nm} &\rightarrow F_3 \approx 0.125, \end{aligned}$$

then there is only one value of ℓ near the expected nominal length that can account for all of these specific fractions. Thus ℓ can be determined uniquely by analysing the fractions. This technique is called ‘the method of excess fractions’¹ [9, 10]. Some details will follow that constrain the uniqueness of the solution, but the above description is the basis of the method, which is described mathematically by the following general expression:

$$\ell = m_1 \frac{\lambda_1}{2} = m_2 \frac{\lambda_2}{2} = \dots = m_i \frac{\lambda_i}{2}, \quad (3)$$

where m_i are interference orders with integer κ_i and fractional F_i parts,

$$m_i = \kappa_i + F_i. \quad (4)$$

Solution of equation (3) for the value of length ℓ follows from knowledge of the wavelengths of light used to measure fractional interference orders of the gauge block.

2.3 Searching For a Fit

The method of excess fractions depends on reliable knowledge of ℓ . In principle, the length could be determined by solving the set of homogeneous equations; however, even if the fringe fractions were measured

¹also ‘method of exact fractions.’

Source	Colour	Vacuum Wavelength λ_v [nm]	1 σ Uncertainty $u(\lambda_v)$ [ppm]
He-Ne Laser	red	632.991 162	0.01
¹¹⁴ Cd Lamp	red	644.024 80	0.03
	green	508.723 79	0.03
	blue	480.125 21	0.03
	violet	467.945 81	0.03

Table 1: Optical sources used in gauge block calibration at NRC and their associated uncertainties.

perfectly, solving equation (3) results in numerous solutions. Moreover, sets of these solutions repeat at a regular length interval (or the synthetic wavelength) [11, 12, 13], which is dictated by the wavelengths of light used in the measurement. There are many possible solutions about the nominal length to choose from, but only one has the best fit to the characteristic fractions; ideally, the correct one. Unfortunately, measurement noise disturbs the sensitive multi-peaked function, causing weaker discrimination amongst the many false solutions, promoting possible selection of an extraneous solution. It has proven to be more reliable to scan through all of the possible lengths in the region of the nominal value, checking the expected fractions to those observed, and picking the length that gives the best overall accounting for the observed fractions. For the 5 wavelengths used in the NRC system, ℓ must be known to within 10 μm . This range of reliability depends on a number of factors, which include the number of wavelengths used, their relative values, and the uncertainty with which the fractions are measured. Generally speaking, the more wavelengths used the better. The electrodeless cadmium-114 lamp provides four CIPM-recommended wavelengths in one convenient source without requiring calibration as the commercially available lasers do. The manufacturers of high grade gauge blocks carefully attend to staying within the specifications of the grade, but occasionally a way out-of-spec block (such as a mis-labelled L value) slips by. This block will likely get weeded out during its first attempt at calibration — the algorithm choosing an alarming value for ℓ .²

At NRC, the length evaluation based on equation (3) is performed by a regression-style computer program. The measurement begins by measuring fringe fractions F_{M,λ_i} (see Figure 3) for each of five wavelengths λ_i . NRC uses the light sources given in Table 1. Fringe fractions are measured in laboratory air for the true length of the gauge block, which is close to the nominal length. The *excess* fractions F_{λ_i} representing the deviation from nominal length d , corrected for the influence of the refractive index of air (see §2.5) are calculated from the measured fractions. The computer algorithm begins with a test length, based on the excess fraction measured for the reference wavelength (NRC chooses the 633 nm laser wavelength). The program steps through test lengths by adding integral interference orders of the reference wavelength κ_r , searching for a minimum of $F_{\lambda_i} - \hat{F}_{\lambda_i}$ summed over all the wavelengths used in the measurement. At each test length, the residual $F_{\lambda_i} - \hat{F}_{\lambda_i}$ is calculated, where F_{λ_i} is the measured excess fraction, and \hat{F}_{λ_i} the excess fraction calculated based on the test length.

The value for the deviation from nominal length then has the form of:

$$d_{fit} = F_{\lambda_r} \frac{\lambda_r}{2} + \kappa_r \frac{\lambda_r}{2} + \left(\frac{\sum_i (F_{\lambda_i} - \hat{F}_{\lambda_i})}{n} \right) \frac{\lambda_r}{2} \quad (5)$$

where $F_r \lambda_r / 2$ is the length equivalent of the reference wavelength excess fraction, $\kappa_r \lambda_r / 2$ is the length equivalent of the number of integral orders stepped through the program, and $(\sum_i (F_{\lambda_i} - \hat{F}_{\lambda_i})) / n$ is the

²The only fail-safe approach is to make a crude length check first, to a few micrometres. This need only be done one time.

mean of the residuals for the $n = 5$ wavelengths used in the NRC measurement. The use of the mean residuals is an important, but subtle, point.

Finally, other instrument and environmental corrections are introduced, so that the calibrated deviation from nominal length of the gauge block is:

$$d = d_{fit} + (20 - t_g)\alpha L + \phi + \Omega L, \quad (6)$$

where ΩL is the obliquity correction, ϕ is the phase-change correction, t_g is the temperature of the gauge block during the measurement and α is the thermal dilatation coefficient for the gauge block material. These corrections are explained in the paragraphs that follow.

2.4 Correction for Thermal Dilatation

Most objects change size with temperature, anywhere from 1 to 50 ppm per Celcius degree,³ depending on the material. To suppress this variable, gauge block length is reported referenced to 20°C in accordance with temperature standard ISO 1 (1975) [8] for dimensional measurements. A correction is applied to account for any difference in length corresponding to the gauge block temperature deviation from 20°C at the time of measurement. This correction is potentially the dominant one, depending on laboratory conditions and practices. Significant uncertainty components also ensue from thermal effects on the gauge unless temperature is well controlled. For steel gauges the thermal dilatation is on the order of 10^{-5} ppm/°C, which corresponds to a correction of about 1 μm on a length of 100 mm, for a gauge temperature deviation of 1°C. NRC uses the thermal dilatation coefficient supplied by the manufacturer without further verification, unless the client specifically requests its evaluation. In the newly renovated NRC labs, the temperature deviation of the gauge block from 20°C is typically less than 0.05°C. In the case of hardened steel, $\alpha = 11.5 \times 10^{-6}/^\circ\text{C}$, and the correction due to thermal dilatation, assuming a gauge temperature deviation of 0.05°C, is $(20 - t_g)\alpha L = 0.6L$ nm, for L in millimetres.

2.5 Correction for the Refractive Index of Air

As mentioned above, the vacuum wavelengths given in the *Mise* are adjusted for the refractive index of air. NRC applies Edlén's equation for the dispersion for dry standard air [14] as modified by Birch and Downs [15] incorporating increased atmospheric carbon dioxide levels and the currently accepted ITS-90 temperature scale:

$$(n_s - 1) \times 10^8 = \left(8342.54 + \frac{2406147}{130 - \gamma^2} + \frac{15998}{38.9 - \gamma^2} \right), \quad (7)$$

where n_s is the index of refraction of standard air, and $\gamma = 1/\lambda$ is the vacuum wavenumber (in μm^{-1}). This equation assumes the carbon dioxide content to be 450 ppm, and no further correction is made for departures from this assumed concentration. The density correction for normal air in the Edlén equation has also been modified to reflect SI units and the ITS-90 temperature scale [16], and is given by:

$$(n_{tp} - 1) = (n_s - 1) \left(\frac{p}{96095.43} \right) \left(\frac{1 + 10^{-8}(0.601 - 0.00972t)p}{1 + 0.0036610t} \right), \quad (8)$$

where n_{tp} is the index of refraction of air, at pressure p in Pascals and temperature t in degrees Celcius. NRC applies the following revised water vapour correction recommended by Birch and Downs [15]:

$$(n_{tpf} - n_{tp}) \times 10^8 = -f(0.037345 - 0.000401\gamma^2), \quad (9)$$

³ppm: parts per million = 10^{-6}

where n_{tpf} is the index of refraction of moist air, and where f is the vapour partial pressure of water in Pascals. The vapour partial pressure f is related by definition to the saturation vapour pressure f_s and the relative humidity by $R \equiv (f/f_s) \times 100$, where R is the relative humidity in percent. NRC calculates f_s from a quadratic function of temperature fitted through saturation pressure values spanning room temperature from the 1984 NBS/NRC Steam Tables [17], such that:

$$f = R(8.753 + 0.036588t^2). \quad (10)$$

Collecting these equations together gives the following empirical equation used in interferometric gauge block measurements at NRC to compensate for the refractive index of air:

$$(n_{tpR} - 1) \times 10^8 = \left(8342.54 + \frac{2406147}{130 - \gamma^2} + \frac{15998}{38.9 - \gamma^2} \right) \left(\frac{p}{96095.43} \right) \left(\frac{1 + 10^{-8}(0.601 - 0.00972t)p}{1 + 0.0036610t} \right) - R(8.753 + 0.036588t^2)(0.037345 - 0.000401\gamma^2). \quad (11)$$

The correction for the refractive index is about $300L$ ppm for $\lambda = 633$ nm, in 20°C air at an atmospheric pressure of 101 kPa and 44% relative humidity. This corresponds to a correction of $300L$ nm for L in millimetres (or 300 nm on 1 mm). The measurement uncertainty attributed to the empirical equation for the refractive index is small (0.01 ppm); however the main contributors to the length dependent uncertainty are a result of measuring the environmental parameters, and for the NRC system amounts to $0.2L$ nm for L in millimetres. Its breakdown is listed in Table 2. Reducing this uncertainty calls for stable laboratory conditions and very low uncertainty measurements of air temperature, pressure and relative humidity.

2.6 The Phase Change Correction

Light reflects from the surface of a dielectric material, like quartz, with a 180° phase change. For other materials, such as metals, the reflected light wave has a phase change different from that of 180° , analogous to a penetration into the surface by a characteristic amount [18, 19, 20]. The optical reflection phase-change correction accounts for this difference in apparent optical penetration of the steel gauge block compared to that of the quartz flat. This correction is somewhat dependent on the wavelength of light; however, at NRC the phase change is treated as an average bias on all the fractions, just as if the gauge were a little shorter and made of quartz. The evaluation of the length is performed without altering the measured fractions for this correction; instead an average phase change correction is applied to the final length solution.

That being said, the phase change correction is actually one of the largest corrections to absolute length measurement by interferometry. As an example of its magnitude, consider a thin high-grade chromium carbide gauge block wrung onto a quartz flat. The gauge may have a length deviation from the nominal of up to 30 nm, with a 2σ calibration uncertainty of 20 nm — but the correction for the phase difference for a chromium carbide gauge wrung to quartz is on the order of 60 nm. The uncertainty attributed to this correction is also one of the largest contributors to the uncertainty budget for the interferometric measurement [21] (see Table 2).

In addition to the above-described optical effect, which is dependent on gauge material (steel, chromium carbide, tungsten carbide, ceramic, etc.), surface characteristics such as roughness, can also alter the phase of the light on reflection. At NRC, material and surface effects are taken as a combined value, and the net phase change correction is measured in the pack experiment⁴ described below. This method assumes that all the gauges within a set are of like material and finish so that they have a common phase correction. For high grade gauge blocks, this is a valid assumption.

⁴also called ‘stack’ experiment by some authors

In the pack experiment, several gauges of good geometry are selected and measured individually, then wrung together in a pack and measured as a unit. The difference in the measured length of the pack as a unit, and the measured lengths of the individual gauges summed together, yields the phase correction. The length of a gauge block can be written in the form of the apparent length, or optical length $l_{0,i}$ given by the optical interference, plus the length equivalent of the phase change difference between the surfaces of the gauge block and the optical flat,

$$l_i = l_{0,i} + \phi. \quad (12)$$

Similarly, for a number of gauges wrung together as a pack, the length of the pack as a unit l_p will be the optical measurement of the pack $l_{0,p}$ plus the phase change correction:

$$l_p = l_{0,p} + \phi. \quad (13)$$

The length of the pack can also be determined by summing the individual measurements l_i of each of the n gauge blocks comprising the pack:

$$l_p = \sum_{i=1}^n l_{0,i} + n\phi. \quad (14)$$

Equating (13) and (14) and rearranging, the phase change correction from the pack experiment is given by

$$\phi = \frac{1}{n-1} \left[l_{0,p} - \sum_{i=1}^n l_{0,i} \right]. \quad (15)$$

It is emphasized that for a reliable evaluation of the phase change correction from pack experiments, the geometry and wringing of the blocks making up the pack must be of superior quality in order to minimize their effects on the overall length of the pack, and hence the phase change correction. Likewise, a high level of confidence in the length measurements of the individual gauges comprising the pack is also desirable. Phase change corrections relative to NRC quartz flats range in value from about 45 nm for ceramic gauge blocks to about 60 nm for chromium carbide gauge blocks. This is an end-effect correction, independent of length.

2.7 The Obliquity Correction

An ideal collimator would have a point source on the optical axis of the lens. In a real system, the source has a finite size (such as an aperture of diameter a) and may be off-axis (oblique) by an amount x . The non-perfect collimation as a result of these imperfections manifest an effective phase distortion. In an interferometer with circular apertures, the obliquity correction is given by:

$$\Omega L = \left(\frac{x^2}{2f^2} + \frac{a^2}{16f^2} \right) L, \quad (16)$$

where f is the collimator lens focal length [22]. The NRC interferometer has a relatively large collimator aperture (as described in the next section), but the corresponding value for the finite aperture size correction, $a^2 L / 16f^2 = 0.105L$ nm for nominal length L in millimetres, is known with a small uncertainty (Table 2, source size). The large aperture diameter is needed for a bright interference image when lamps are used. The interferometer has provision for the alignment of the telescopes so that the entrance fibre end source and the exit aperture may be superimposed. Such alignment is performed at the beginning of each gauge measurement to ensure that the entrance and exit apertures are indeed co-incident with the optic axis of the interferometer, therefore correction $x^2/2f^2$ is nominally zero, and the associated uncertainties are kept small (Table 2, alignment).

3 Gauge Block Interferometer Apparatus

The NRC Gauge Block Interferometer (GBIF) is a Michelson interferometer modified to use collimated light (Twyman-Green configuration). Using collimated light ensures that interference fringes always have equal thickness, irrespective of the optical path distance (OPD) between the reference surfaces of the instrument. In the following paragraphs, the main components are referred to by symbols shown in Figure 4.⁵

The GBIF is housed in a newly-renovated environmentally-controlled laboratory. The laboratory is designed such that temperature is $20 \pm 0.1^\circ\text{C}$ throughout the lab, and relative humidity is controlled to $40 \pm 2\%$. Moist air can rust instruments and gauges; drier air is unpleasant and fosters static electricity problems.

Two light sources provide the stable frequencies with traceability in accordance with the CIPM “*Mise en Pratique* of the Definition of the Metre (1992)” [1]. A commercially available polarization-stabilized single frequency He-Ne laser (Coherent Tropol, Model 200) is calibrated at NRC against an iodine-stabilized He-Ne laser operating in accordance with the *Mise*. The other light source currently used at NRC is an electrodeless cadmium-114 lamp operating in accordance with CIPM recommendations [23]. This lamp is a bright source that is relatively easy to operate. It is excited by microwave energy (Ophos Instruments Inc., Model MPG4) and produces four lines: red, green, blue and violet. Note that these spectral radiations appear in the CIPM “List of Recommended Radiations, 1983”, meaning that they too can be used as direct ‘realisations of the metre according to its internationally accepted definition,’ and thus do not require further calibration to establish traceability to the definition. Table 1 summarizes the wavelengths used in gauge block calibrations and their associated uncertainties.

The light sources are arranged on a remote table (ST in Figure 4), so that their heat does not perturb the interferometer. At present, the cadmium-114 lamp and He-Ne 633-nm laser are in use (Cd and L1 in the figure); the other lamps are off-line, and new lasers are queued to be installed in 1Q/1997 (only L2 is shown). The sources are directed onto a selection mirror SM, which can be indexed from the operator console to point to the desired light source (remote control actuators are shown as generic motors M throughout Figure 4). The filter wheel FW is needed to select one-at-a-time the four wavelengths emitted by the cadmium-114 lamp. Special high-efficiency interference filters for separating the cadmium-114 wavelengths were recently designed and fabricated by the NRC Thin Films Group, and installed in our system. A microscope objective OB focuses the selected radiation onto the end of an optical fibre OF, which conveys the light about 3 m to the interferometer. The fibre is 0.6 mm in diameter, the large size being needed to admit sufficient light from the relatively weak, poorly collimated cadmium-114 lamp (compared to that from the laser). The fibre is made to touch a small buzzer V that quietly vibrates enough to wash out any speckle pattern when the laser source is selected.

The fibre is aligned at the other end to serve as a point-source for the GBIF entrance collimator C1 (*i.e.*, on-axis and at the focus of the collimator). Its 0.6mm diameter flat-lapped tip behaves as a uniformly-illuminated aperture, whose finite size and possible misalignment must be accounted for in the obliquity corrections (§2.7) and the uncertainty calculation (§5). The entrance collimator has a focal length of 463 mm, and limits the aperture of the optical system to about 80 mm diameter. The exit collimator C2 has matching properties, and both view the interferometer via port windows W in the walls of the hermetic enclosure HE of the instrument. The angular alignment of each collimator with respect to the interferometer reference surfaces can be fine-tuned by remote control (M).

The optical path of the interferometer is shrouded against air turbulence and changing laboratory conditions. Beam tubes are used for the entrance and exit telescopes, and Figure 4 shows that most of the interferometer components are within the hermetic enclosure HE. The enclosure is a thick-walled aluminum shroud, which

⁵NRC does not promote or endorse any of the products or services named in this article.

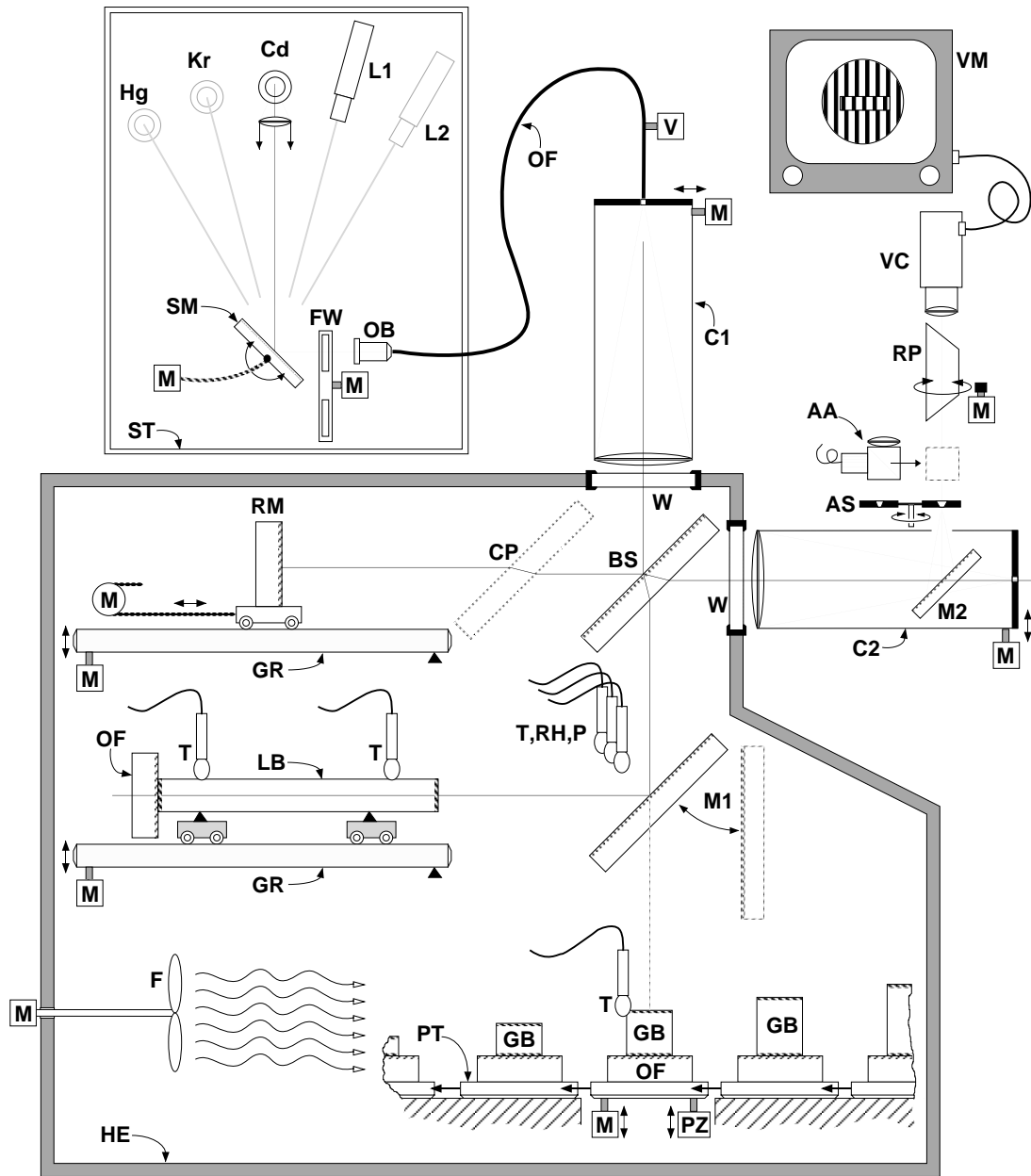


Figure 4: Schematic of NRC Gauge Block Interferometer, comprised of: source table ST; isotope lamps cadmium (Cd), krypton (Kr), mercury (Hg); lasers L1, L2; selecting mirror SM; remote-control motors M; filter wheel FW; microscope objective OB; optic fibre OF; vibrator V; entrance and exit collimators C1, C2; hermetic enclosure HE; port windows W; beam splitter BS; compensator plate CP; reference mirror RM; guide rails GR; length bar LB; optical flats OF; temperature, relative humidity and pressure sensors T, RH, P; removable mirror M1; gauge blocks GB, pallet PT, piezo positioners PZ; fan F; turning mirror M2; aperture selector AS; autocollimation aid AA; rotation prism RP; video camera VC; video monitor VM. The components are explained in detail in the text.

seals to the thick slab of machined aluminum that serves as the foundation for the interferometer. The seal allows minute pressure adjustments (useful for setting a ‘zero-fringe-fraction’ condition in long bar calibrations), and even total evacuation (to eliminate effects of index of refraction). The high thermal conductivity and low emissivity of the assembly promotes a uniform, stable temperature within the enclosure. The GBIF is thermally passive: the internal temperature is not controlled, but rather moderates the excellent ambient conditions in the lab and is carefully measured by several sensors (\mathbb{T}) monitoring both the inside air and the gauge temperature, for subsequent calculated corrections. The absolute temperature is measured with a combined uncertainty of 3 mK to a resolution of 1 mK (0.001°C). Typical air temperature drift is less than 10 mK per hour. The bead-in-glass thermistors (VECO, SensiChip) are calibrated by Thermometry at NRC. A slow-turning fan blade \mathbb{F} gently stirs the air within the enclosure to prevent thermal stratification. Its motor runs full-time and is outside the enclosure; other alignment motors within the enclosure run only in tiny bursts from time-to-time, and have a negligible effect on the temperature. Gauge temperature is probed by attaching a thermistor to a sample gauge block in the neighborhood of the test arm of the interferometer. Pressure \mathbb{P} and relative humidity \mathbb{RH} are also measured within the enclosure, to allow calculated corrections to the index of refraction of the air. Air pressure is measured using an MKS Baratron capacitance manometer (Model 310BHS-1000), calibrated by Mechanical Metrology at NRC. Air pressure drift during gauge block measurements generally follows the ambient atmospheric conditions. The relative humidity sensor (Vaisala HUMICAP Model HM132-O0052-1.2) is calibrated in our lab against a chilled mirror hygrometer (General Eastern Dew Point Monitor, Model HYGRO-M1, Sensor Model 1111H).

Referring to Figure 4, the reflected and transmitted collimator axes are aligned to be collinear at the primary surface of the beamsplitter \mathbb{BS} . The entrance beam divides at \mathbb{BS} , the reflected portion going to the reference mirror \mathbb{RM} , and the transmitted portion going to the gauge block \mathbb{GB} and optical flat \mathbb{OF} ensemble. Reflected wavefronts from the reference mirror and the gauge/flat ensemble combine (interfere) at the beamsplitter, and the interfering beams are directed into the exit collimator $\mathbb{C}2$, turned at mirror $\mathbb{M}2$, and passed on to the viewing system. An aperture selector \mathbb{AS} positions a 0.6 mm diameter aperture to restrict the exit pupil to be on-axis and at the focus of $\mathbb{C}2$. A rotatable dove prism \mathbb{RP} allows the operator to conveniently orient the image of the interference pattern captured by the CCD video camera \mathbb{VC} and viewed on the video monitor \mathbb{VM} . The camera has a two-stage image intensifier to brighten the dim images from isotope lamps, and a digital video processor captures 32 frames as an average image, to further improve the S/N ratio.

The autocollimation aid \mathbb{AA} shown in the figure consists of a beamsplitter, an LED light source and a lens that brings the aperture selected in \mathbb{AS} into focus on the video monitor. When this assembly is slid into position, $\mathbb{C}2$ can be autocollimated (*i.e.*, the light from the LED passed backwards through the aperture and collimator is reflected by the reference mirror \mathbb{RM} , returns through the collimator and is re-imaged in the aperture, like an eclipse). By making the eclipse appear ‘full’, $\mathbb{C}2$ can be brought into optimal angular alignment, a crucial step to control this component of the measurement uncertainty.

Figure 4 attempts to depict some of the mechanics of the instrument, in particular the transport, support and alignment of the gauges and reference mirror. Long bars (gauges) up to 1 m are supported horizontally by a pair of carriages that can be positioned along a stiff guide rail \mathbb{GR} . A small optical flat \mathbb{OF} is wrung to the far end of the bar to provide the reference surface for that end, and the support carriages are positioned at the effective Airy points (normally $0.211 L$ from the ends, adjusted for the end-load of the optical flat) such that the bar ends remain parallel in the presence of bar-bending due to gravity. Fine angular alignment is made from the console by motors that act on the guide rail.

A matching rail system supports the reference mirror \mathbb{RM} , with the additional feature that \mathbb{RM} can be transported along the length of the rail. The reference mirror position is adjusted prior to the measurement of each gauge so that the OPD of \mathbb{RM} is roughly midway between the OPDs of the front and back surfaces of the gauge. This becomes important on longer gauges when using isotope discharge lamps, since this radiation has a short coherence length (about 100 mm for cadmium-114), and the interference fringe visibility degrades

as the optical path differences approach the coherence length of the light. Calibrating longer bars (over 200 mm) with isotope lamp radiations is especially tedious, as the front and back surfaces of a calibrated shorter gauge is used as an ‘extended reference mirror’ to interfere with the respective front and back surfaces of the longer bar, thereby extending the range by the coherence length at the front and at the back of the shorter gauge (for example, using cadmium-114’s 100 mm coherence length, one could use a 200 mm gauge to calibrate to 400 mm, the 400 mm to do 600 mm, and so on to 800 mm, and finally 1 m). The krypton-86 source has longer coherence length, allowing fewer steps, but is more cumbersome to operate (immersed in liquid nitrogen maintained at the triple-point temperature). Such techniques are not needed for laser sources, with their metres of coherence length, and NRC is installing two more He-Ne lasers (612 nm and 543 nm) to augment the 633 nm unit to facilitate long bar calibrations.

Figure 4 also shows a (future) compensator plate CP in the reference arm of the interferometer. This component is needed for the reference beam to match the path through quartz taken by the gauge beam, which makes two extra passes through the thickness of the quartz beamsplitter BS. This compensation is only needed for white light interferometry (where OPDs must be matched achromatically), and CP is queued to be installed in 1Q/1997 as NRC gears up for research in this area.

Each short gauge block is wrung to a quartz optical flat 25 mm thick \times 75 mm diameter. Quartz is used so that wringing can be inspected from underneath. The large aspect ratio of the flats maintains the integrity of the flatness in the presence of bending forces (wringing and support of the gauge load). These flats have been verified by the Optics Group at NRC to have flatness better than 30 nm in the central region.

The last aspect of Figure 4 deals with short gauge blocks (GB). A removable mirror M1 allows manual switching between long-bar and gauge-block modes. Generally, only one long bar measurement can be done in a day, so any manual switching can be done during the set-up of the long bar. The gauge block conveyor can be loaded with up to 18 gauges at a time, the enclosure sealed, and subsequent transport, alignment and measurement all done by remote control. A gauge block wrung to the optical flat is placed on a square pallet PT. The base of the interferometer has a shallow channel cut in the top surface as a raceway to contain and guide two rows of nine pallets each in a rectangular circuit, all within the enclosure and remotely controllable. One of the corners of the circuit (where a pushed pallet comes to rest after the conveyor cycle) is arranged so that a gauge block/optical flat ensemble is in the field of view of the interferometer. A tip/tilt piezo positioner PZ allows the operator to make fine adjustments to the fringe pattern as each gauge is cycled into position.

4 Measurement Procedure

4.1 Inspection and Wringing

Each gauge block is first cleaned with solvent to remove any rust-inhibiting coating, and then inspected for defects in the gauging surfaces that might interfere with measurement or potentially damage the optical flat. A minute film of wringing oil is applied to one of the reference surfaces by dabbing a smudge of non-corrosive, light textured oil⁶ and polishing the surface until it appears to be clean with a lint-free tissue. This surface of the gauge block is then wrung to the centre of a carefully cleaned quartz optical flat by placing the flat over the block, which is resting on the bench surface wringing-side up. The flat is first contacted at an angle on an edge of the block, then is rolled onto the gauge block in a twisting motion to force out the air film. The wringing film is very thin and, with practise, very reproducible. The quality of the wring is judged by

⁶Products containing silicon are avoided as they are very difficult to remove completely.

viewing through the under side of the optical flat for a uniformly wet look indicating uniform contacting of the gauge, free of specks or interference fringes.⁷ A correctly wrung gauge block has a wringing film about 10 ± 5 nm in thickness; the block is tightly adhered, difficult to slide and position, and the two can be handled as a single unit. Thin gauges conform to the shape of the optical flat. Considerable skill is needed to wring the gauge tightly, centred on the flat, with minimal temperature distortion of the gauge block. The wrung gauge blocks are loaded into the GBIF one at a time, in a vertical orientation, and allowed to thermally stabilize overnight.

4.2 Gauge Measurement

The next day, each gauge is conveyed in turn into the measuring position and optical alignment of the interferometer is verified. For each wavelength, the fractional difference between the fringe pattern formed on the gauge and that formed on the optical flat (see Figure 3) is measured with the aid of a video system and a fiducial allowing precise pointing to the fringe center. Air temperature, pressure, relative humidity and gauge temperature are probed and recorded by the computer for use in the on-line evaluation of the gauge length. Gauge geometry is quickly evaluated by eye for each gauge. If the non-flatness or non-parallelism are significant enough to alter the central length measurement, flatness and parallelism measurements are taken at this time. Reading the five fringe fractions for the central length measurement takes about 5–10 minutes. Drift in any of the environmental conditions under the interferometer enclosure during the measurement time interval is negligible.

Once the fringe fractions for the five reference wavelengths of light and the environmental conditions have been recorded, the length of the gauge is evaluated on-line by the computer program as described above. The on-line length evaluation permits re-measuring immediately if a problem is suspected, saving unnecessary repetition of time-consuming wringing and set-up of the gauges. All corrections except the phase change correction are applied in this step. Reading repeatability depends on the gauge quality, but is usually less than 10 nm.

Following measurement, gauge blocks are cautiously removed from the optical flats by heating the gauge with the fingers and sliding, or by lightly tapping the side of the gauge with a brass rod, allowing the vibrations to break the wring. Gauges are de-magnetized and given a rust-inhibiting coating.

Following this initial interferometric measurement of all the gauges in the set, four gauges with good geometry and in the nominal length range of 5–10 mm are selected to measure the phase change correction. These selection criteria attempt to minimize the effects of wringing and thermal dilatation on the phase change correction evaluation.

4.3 Check Gauges

NRC check gauges are included in each measurement run to monitor the system performance. The measurement reproducibility observed for the central length measurement of a 10 mm gauge block is 20 nm (2σ standard deviation). This result represents measurements spanning a two year period of various operators measuring both sides arbitrarily, under typical laboratory conditions. Several check gauges are rotated in routine measurements. The quality of gauge geometry is observed to have a significant affect on the repro-

⁷Correct conditions are paramount to obtain proper wringing: the most minute particle of dust can prevent the faces from wringing together, and on the other hand, contacting very flat, highly-polished, clean surfaces can result in a wring so tight that subsequent attempts to separate the pieces could damage the surfaces if special precautions are not taken.

ducibility of central length measurements, primarily due to wringing variations. Some gauges even display a different central length when wrung to one side as compared to the other (a 40 nm difference has been observed).

The algorithm embodied in the computer program has been in place since 1982. Gauge block measurements performed with this system have consistently agreed in comparisons with other laboratories. The most recent comparison with the NORAMET national laboratories reiterates this excellent agreement [24].

5 Evaluation of Measurement Uncertainty

The measurement uncertainty is evaluated in accordance with the *Guide to the Expression of Uncertainty in Measurement* [25]. The *Guide* groups statistical evaluation of uncertainty as Type A, and other forms of uncertainty assignment as Type B. The combined standard uncertainty in the interferometric measurement of a gauge block is a quadrature sum of uncertainty components attributed to factors which influence the measurement. Uncertainties are based on characterisation experiments performed in-house on the NRC gauge block interferometer, calibration data from other NRC laboratories, and manufacturers specifications. The detailed calculation has been described in [21]. Values listed in Table 2 are the standard uncertainties (1σ) attributed to these influence factors. Length dependent and end-effect uncertainties are summed separately in quadrature for the expanded combined uncertainty U in the interferometric gauge block measurement. The quadrature sum can be approximated in a more convenient linearized form, $U = (19 + 0.28L)$ nm, for nominal length L in millimetres, and a coverage factor of $k = 2$.

Scrutinizing the evaluation of the measurement uncertainty revealed aspects of NRC practice where improvements could be implemented. For example, now that the temperature is so well controlled in the new laboratory, Table 2 shows that the air pressure sensor has emerged as the dominant source of uncertainty. A better pressure sensor has been ordered ($u(p) \sim 10$ Pa).

6 Future Improvements

Plans are underway to upgrade the NRC gauge block interferometer by applying phase-shifting methods to the interference fringe fraction analysis. Automating the interference fraction evaluation will increase the accuracy of the fringe fraction measurements, and relieve the operator from a tedious task. Additional He-Ne lasers stabilized at 612 nm, 543 nm and 594 nm have been purchased, and will facilitate long-bar calibration to be brought back on-line. A new beam splitter and compensator plate have been made in-house by the Optical Component Laboratory and are queued to be installed. These components will offer improved wavefront quality, and allow experiments in white-light interferometry to be undertaken on this same instrument. NRC also has plans to set up a facility for fabricating electrodeless cadmium-114 lamps in-house. For short gauge blocks, the cadmium-114 lamp remains a convenient source of four wavelengths.

Influence Factor x_i	Physical Standard Uncertainty $u(x_i)$	Contribution to Length Uncertainty $c_{x_i}u(x_i)$ [nm]
Fraction measurement (Type A)	0.004 fringe	1.4
Wringing (Type A)	6 nm	6
Phase-change	6 nm	6
Gauge block flatness and parallelism	2 nm	2
Interferometer optics:		
Wavefront errors	3 nm	3
Obliquity:		
source size	5 μm	0.002 L
alignment	50 μm	0.008 L
He-Ne laser:		
1-year drift	0.01 ppm	0.005 L
calibration	0.002 ppm	0.001 L
Lamp wavelength	0.02 ppm	0.0002 L
Thermal dilatation coefficient [†]	0.7 ppm/K	0.033 L
Gauge temperature [†] :		
sensor calibration	2.5 mK	0.029 L
gauge gradient	5 mK	0.058 L
reading capability	0.1 mK	0.001 L
cross term		0.004 L
Refractive Index of Air:		
Edlén's equation	0.01 ppm	0.010 L
Air pressure		
calibration	50 Pa	0.135 L
reading capability	4 Pa	0.011 L
drift	54 Pa	0.146 L
Air temperature		
calibration	2.5 mK	0.004 L
reading capability	0.1 mK	0.0001 L
drift	1 mK	0.001 L
Humidity		
accuracy	1.2%	0.010 L
reading capability	0.1%	0.001 L
drift	1%	0.009 L
Quadrature Sum:		$9.3^2 + 0.21^2L^2$ nm ²
Linearized Expanded Uncertainty:		$19 + 0.28L$ nm

ppm: parts per million = 10^{-6}

[†]Assumes steel gauge block, $\alpha = 11.5$ ppm/K.

Table 2: Standard uncertainties attributed to the measurement of gauge blocks in the NRC gauge block interferometer, where L is in millimetres. A coverage factor of $k = 2$ is used for the expanded uncertainty. All uncertainty evaluations are Type B, except where noted in the table.

7 Conclusion

The NRC gauge block interferometer was described. The measurement procedures used in the interferometric measurements and the associated uncertainties were outlined. With this procedure, a single operator is able to perform absolute measurement of 5–10 gauge blocks a day to an uncertainty of $U = (19 + 0.3L)$ nm, where L is in millimetres.

8 Acknowledgements

The authors would like to thank the expert technical assistance of L. Munro for design improvements to the interferometer and maintenance of the metrology laboratory environmental conditions, and R. Thibedeau for gauge measurements. The authors also thank NRC colleagues A. Agarwal, A. Bass, D. Lawlor and D. Gee for traceable sensor calibrations.

References

- [1] Quinn, T.J., 1994, “*Mise en Pratique* of the definition of the metre (1992),” *Metrologia*, **30**, pp. 523–541.
- [2] Middleton, W.E.K., 1979, *Physics at the National Research Council of Canada 1929–1952*, (Wilfrid Laurier University Press, Waterloo, Ontario), pp. 44–50, and pp. 105–110.
- [3] Baird, K.M., 1957, “Calibration of Gauge Blocks in Canada,” Proceedings of a Symposium on Gage Blocks held at NBS on 11–12 August 1955, National Bureau of Standards Circular 581, pp. 21–25.
- [4] Pekelsky, J.R., 1991, “Length Standards at the National Research Council of Canada,” NCSL 11th Annual Canadian Workshop and Symposium, 9–10 October 1991, Canada Centre for Inland Waters, Burlington, Ontario, 14 pages. [NRC 33075]
- [5] Baird, K.M., 1963, “Vacuum wavelengths of Kr^{86} , Hg^{198} , and Cd^{114} ,” *Jour. Opt. Soc. Amer.*, **53**(6), pp. 717–720. [NRC 7359]
- [6] Hanes, G.R. and Dahlstrom, C.E., 1969, “Iodine hyperfine structure observed in saturated absorption at 633 nm,” *Appl. Phys. Letters*, **14**(11), pp. 362–364. [NRC 3249]
- [7] Hanes, G.R. and Baird, K.M., 1969, “ I_2 controlled He-Ne laser at 633 nm: preliminary wavelength,” *Metrologia*, **5**(1), pp. 32–33.
- [8] ISO 3650–1978(E), 1988, *ISO Standards Handbook 33: Applied Metrology — Limits, fits and surface properties*, 1st Edition, (ISO Central Secretariat, Switzerland), pp. 778–786 and p. 223.
- [9] Born, M. and Wolf, E., 1980, *Principles of Optics*, 6th ed., (Pergamon Press, New York), pp. 286–306.
- [10] Michelson, A.A. and Benoit, J.R., 1895, “Valeur du mètre en longueurs d’ondes,” *Trav. et Mem. Int. Bur. Poids et Mes.*, **11**, p. 1, and Benoit J.R., 1898, “Application des phénomènes d’interférence à des déterminations métrologiques,” *J. de Phys.*, **3**(VII), pp. 57–68.
- [11] Hariharan P., 1992, *Basics of Interferometry*, (Academic Press, Inc., New York), Chapter 8.
- [12] Lewis, A., 1994, “Measurement of length, surface form and thermal expansion coefficient of length bars up to 1.5 m using multiple-wavelength phase-stepping interferometry,” *Meas. Sci. Technol.*, **5**, 694–703.

- [13] Siemsen, K.J., *et al.*, 1997, “A multiple frequency heterodyne technique for the measurement of long gauges,” *Metrologia*, in press.
- [14] Edlén B., 1966, “The refractive index of air,” *Metrologia*, **2**(2), pp. 71–80.
- [15] Birch, K.P. and Downs, M.J., 1994, “Correction to the updated Edlén equation for the refractive index of air”, *Metrologia*, **31**, pp. 315–316.
- [16] Birch, K.P. and Downs, M.J., 1993, “An updated Edlén equation for the refractive index of air”, *Metrologia*, **30**, pp. 155–162.
- [17] Haar L., Gallagher J.S., Kell G.S., 1984, “NBS/NRC Steam Tables: Thermodynamic and transport properties and computer programs for vapor and liquid states of water in SI units,” (Hemisphere Publishing Corp., Washington), p. 9.
- [18] Ciddor, P.E., 1990, “Phase Correction in Gauge Block Interferometry: New Procedures,” CSIRO Australia, DAP Technical Memorandum No. 72, 12 pages.
- [19] Li, T. and Birch, K.G., 1987, “A practical determination of the phase change at reflection,” *IEEE Trans. Instr. Meas.*, **IM-36**(2), pp. 547–550.
- [20] Saunders, J.B., 1957, “A high-sensitivity interferometer for measurement of phase shift and other applications,” Proceedings of a Symposium on Gage Blocks held at NBS on 11–12 August 1955, National Bureau of Standards Circular 581, pp. 51–59.
- [21] Decker, J.E. and Pekelsky, J.R., 1996, “Uncertainty evaluation for the measurement of short gauge blocks by optical interferometry,” National Research Council of Canada (NRC), Ottawa, Canada Report No. 40001, 33 pages.
- [22] Bruce, C.F., 1957, “Obliquity effects in interferometry,” *Optica Acta*, **4**, pp. 127–135, also Engelhard, E., in “Metrology of Gauge Blocks,” *National Bureau of Standards Circular 581*, 1 April 1957, pp. 1–20.
- [23] *Comité Consultatif pour la Définition du Mètre*, 3rd session, 1962, pp. 18–19 and *Procès-Verbaux CIPM*, 52nd session, 1963, pp. 26–27.
- [24] Decker, J.E., *et al.*, 1997, “NORAMET comparison of gauge block measurement by optical interferometry,” *Metrologia*, to be published.
- [25] “Guide to the expression of uncertainty in measurement”, 1993, 1st Edition (International Organization for Standardization, Switzerland), 101 pages.